Broadband and omnidirectional antireflection employing disordered GaN nanopillars

C. H. Chiu,[1] Peichen Yu,[1,*] H. C. Kuo,[1] C. C. Chen,[1] T.C. Lu,[1] S. C. Wang,[1] S. H. Hsu,[2] Y. J. Cheng,[2] and Y. C. Chang,[2]

[1] *Department of Photonics and Institute of Electro-Optical Engineering, National Chiao-Tung University, Hsinchu, Taiwan, R.O.C.*
[2] *Research Center for Applied Sciences, Academia Sinica, Taipei, Taiwan, R.O.C.*
[*] *Corresponding author: yup@faculty.nctu.edu.tw*

Abstract: Disordered GaN nanopillars of three different heights: 300, 550, and 720 nm are fabricated, and demonstrate broad angular and spectral anti-reflective characteristics, up to an incident angle of 60° and for the wavelength range of λ=300-1800nm. An algorithm based on a rigorous coupled-wave analysis (RCWA) method is developed to investigate the correlations between the reflective characteristics and the structural properties of the nanopillars. The broadband and omnidirectional antireflection arises mainly from the refractive-index gradient provided by nanopillars. Calculations show excellent agreement with the measured reflectivities for both s- and p- polarizations.

©2008 Optical Society of America

OCIS codes: (220.4241) Nanostructure fabrication; (310.6628) Subwavelength structures; (310.1210) Antireflection coatings.

References and links

1. D. S. Hobbs, B. D. MacLeod, and J. R. Riccobono, “Update on the development of high performance anti-reflecting surface relief micro-structures,” Proc. SPIE **6545,** 65450Y-1-14 (2007).
2. G. R. Lin, Y. C. Chang, E. S. Liu, H. C. Kuo, and H. S. Lin, “Low refractive index Si nanopillars on Si substrate,” Appl. Phys. Lett. **90**, 181923-181925 (2007).
3. Y. Kanamori, K.-I. Kobayashi, H. Yugami, and K. Hane, “Subwavelength antireflection gratings for GaSb in visible and near-infrared wavelengths,” Jpn. J. Appl. Phys. **42**, 4020-4023 (2003).
4. Y. Zhao, J. Wang, and G. Mao, “Colloidal subwavelength nanostructures for antireflection optical coatings**”** Opt. Lett. **30**, 1885-1887 (2005).
5. S. Nakamura, M. Senoh, S. Nagahama, N. Iwasa, T. Yamada, T. Matsushita, H. Kiyoku, and Y. Sugimoto, “InGaN-Based Multi-Quantum-Well-Structure Laser Diodes,” Jpn. J. Appl. Phys. **35**, L74-L76 (1996).
6. A. Xing, M. Davanco, D. J. Blumenthal, and E. L. Hu, “Fabrication of. 2-D photonic crystal membrane structure,” J. Vac. Sci. Tech. B **22**, 70-73 (2004).
7. C. C. Yu, C. F. Chu, J. Y. Tsai, H. W. Huang, T. H. Hsueh, C. F. Lin, and S. C. Wang, “Gallium Nitride Nanorods Fabricated by Inductively Coupled Plasma Reactive Ion Etching,” Jpn. J. Appl. Phys. **41**, L910 – L912 (2002).
8. W. Q. Han, S. S. Fan, Q. Q. Li, and Y. D. Hu, “Synthesis of Gallium Nitride nanorods through a carbon nanotube-confined reaction,” Science **277**, 1287-1289 (1997).
9. H. M. Kim, D. S. Kim, T. W. Kang, Y. H. Cho, and K. S. Chung, “Growth and characterization of single-crystal GaN nanorods by hydride vapor phase epitaxy,” Appl. Phys. Lett. **81**, 2193-2195 (2002).
10. H. W. Huang, C. C. Kao, T. H. Hsueh, C. C. Yu, C. F. Lin, J. T. Chu, H. C. Kuo, and S. C. Wang, “Fabrication of GaN-based nanorod light emitting diodes using self-assemble nickel nano-mask and inductively coupled plasma reactive ion etching,” Mater. Sci. Eng. B **113**, 125-129 (2004).
11. Y. Du, S. Han, W. Jin, C. Zhou, and A. F. J. Levi, “Polarization-dependent reflectivity from dielectric nanowires,” Appl. Phys. Lett. **83**, 996-998 (2003).
12. Y. Kanamori, M. Sasaki, and K. Hane, “Broadband antireflection gratings fabricated upon silicon substrates,” Opt. Lett. **24**, 1422-1424 (1999).
13. C.-C. Chen, P. Yu, J.-C. Yu, and H.-C. Kuo are preparing a manuscript to be called “Angular and Spectral Reflectivity Calculations of Silicon Nano-Textured Surfaces.”

#92997 - $15.00 USD Received 28 Feb 2008; revised 29 Mar 2008; accepted 31 Mar 2008; published 30 May 2008

1. Introduction

High performance and cost effective anti-reflective (AR) surfaces enable a variety of applications such as high-power laser systems, imaging cameras, sensor arrays, and solar cells. Over the past decade, the development of AR surfaces employing periodic sub-wavelength structures (SWS) has shown several advantages over the conventional dielectric AR coatings, such as broad angular and spectral responses, polarization insensitivity, and reliability in harsh and abrasive environments [1]. Recently, the interests in nano-scaled AR textures have been extended to disordered structures, where the fabrication cost is significantly reduced without the requirement of the electron beam lithography. Moreover, a variety of materials, including Si, GaAs, and glass [1], are available for the applications, offering versatile device possibilities.

While several studies have been made on the reflectivity characterizations of disordered nanostructures [2-4], few reports have discussed the correlation between the reflective characteristics and the structural properties, such as geometric shapes, dimensions, and densities. Calculations on the reflectivities of nanostructures are also a challenge due to the nature of disorder, hindering further progress in device design and analysis. In this work, we have fabricated GaN nanopillar structures with three different heights: 300, 550, and 720nm. Since GaN is a wide bandgap material [5], the observed AR characteristics can be correlated with the structural properties. An algorithm based on a rigorous coupled-wave analysis (RCWA) method is also developed to investigate the dependence of reflectivities on the structural properties of nanopillars without considering sidewall roughness and scattering. Calculations also show excellent agreement with the measured reflectivities for both s- and p-polarizations.

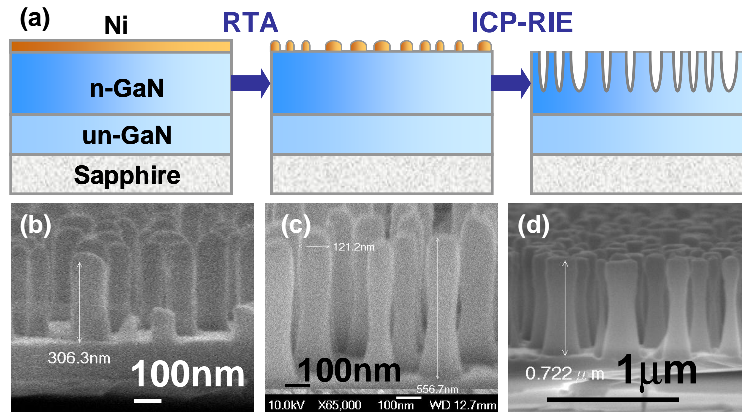

Fig. 1. (a). The schematics of n-GaN nanopillars fabricated using self-assembled Ni nano-masks and ICP-RIE process. Cross-sectional views of the FESEM graphs for fabricated nanopillar structures with heights of (b) 300 nm, (c) 550 nm, and (d) 720 nm.

2. Fabrication and characterization

GaN nanostructures can be fabricated using various techniques, such as E-beam lithography [6], inductively coupled-plasma reactive ion etching (ICP-RIE) process [7], synthesis using carbon-nanotube templates [8], or epitaxial growth of nanostructures [9]. In this work, the GaN nanopillars of different heights were fabricated by a relatively simple method, using self-assembled Ni nano-masks and ICP-RIE process as illustrated in Fig. 1(a). The samples were grown by metal organic chemical vapor deposition (MOCVD) with a rotating-disk reactor on a c-plane sapphire (0001) substrate at the growth pressure of 200 mbar. The epitaxial structure consisted of a 2-μm-thick GaN nucleation layer and a 2-μm-thick Si-doped n-GaN layer. A Ni film with a thickness of 10nm was first evaporated on the n-GaN surface using an E-beam evaporating system, followed by the rapid thermal annealing (RTA) process under the N_2

#92997 - $15.00 USD Received 28 Feb 2008; revised 29 Mar 2008; accepted 31 Mar 2008; published 30 May 2008
(C) 2008 OSA

flowing gas of 10 SCCM at 850 °C for 90 seconds to form Ni nano-dots, served as the etch masks. The diameter, density, and averaged height of the nano-masks were approximately 150 nm, $3x10^9$ cm^{-2}, and 120 nm, respectively. The fill factors of the nano-masks in general can be varied from 33% to 45% by controlling the thickness of the deposited Ni film. The samples were then etched by the ICP-RIE system (SAMCO ICP-RIE 101iPH) operated at 13.56 MHz under a gas mixture of Cl_2/Ar = 45/30 SCCM through individual electronic mass flow controllers. The ICP source power, bias power, and the chamber pressure of the ICP-RIE system were set to 400W, 100 W, and 0.66 Pa, respectively. Finally, the samples were dipped into a heated nitric HNO_3 at 100 °C for 10 min to remove the residual Ni nano-masks. Details of the nanopillar formation process were described in [10]. The diameter and density of the fabricated nanopillars were nearly the same as those of the Ni masks, while the height was controlled by etching time.

We have fabricated GaN nanopillars with heights of h=300, 550 and 720 nm, corresponding to the etching times of 60, 90 and 120 sec, respectively. Figures 1(b) to 1(d) show the cross-sectional views of the field-emission scanning electron micrographs (FESEM) of the fabricated samples. The respective etching rates were approximately 5, 6.11, and 6nm/sec, indicating a slower etching rate at the beginning period due to the unapparent initial bombardment efficiency. However, the etching rate was decreased again at the etching time of 120 sec because, as shown in Fig. 1(c), the lateral etching of nanopillars became noticeable, limiting the etch depth. A deeper nanopillar structure could be achieved if the flow rate of the etching gas (Cl_2) was reduced along with an increase in ICP power. It is found that the flow rate of Cl_2 and ICP power are critical in controlling the shape of nanopillars.

The reflectivity of the n-GaN nanopillars was characterized as a function of the incident angle for both s- and p- polarizations, using a linearly polarized He-Ne laser at λ= 632.8 nm. The incident power was set to 3 mW with a spot size of ~1mm. As shown in the inset of Fig. 2, light struck on the sample at an incident angle θ_i, with respect to the surface normal, while the detector on the other side received the reflected light at the same angle, $\theta_o=\theta_i$. Both angles were varied from 20° to 80°. The system was calibrated with a silicon substrate before measurements. We also verified that the reflectivities contributed by high-order diffractions were negligible. For reflectivity spectroscopy, the incident light was obtained from a monochromator using a xenon lamp with wavelengths ranging from 300 to 1800 nm.

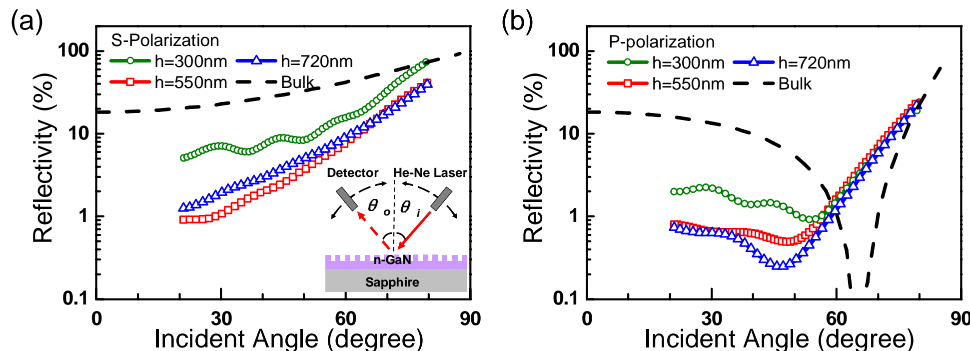

Fig. 2. Measured reflectivities of GaN nano-pillars with three different heights: h=350nm, 550nm, and 720nm, for (a) s-polarization and (b) p-polarization. The inset shows a schematic of the measurement setup.

3. Results and discussion

The measured angle-dependent reflectivities for GaN nanopillars of different heights are shown in Fig. 2(a) for s-polarization and (b) for p-polarization. The calculated reflectivities of bulk GaN (n=2.5) for both polarizations are also plotted for reference. As shown in Fig. 2, the angular reflectivities in GaN nanopillar structures have been drastically reduced from those of bulk. As shown in Fig. 2(a), the reflectivities of s-polarization for h=550 and 720nm are

#92997 - $15.00 USD Received 28 Feb 2008; revised 29 Mar 2008; accepted 31 Mar 2008; published 30 May 2008
(C) 2008 OSA

nearly identical, showing excellent AR characteristics (<3%) up to an incident angle of 50°. The reflectivities for h=330nm are relatively high and the interference from air/GaN and GaN/sapphire interfaces can also be observed. The interference characteristics completely vanish for h=550 and 720 nm, since the scattering on the nanopillar surfaces give rise to phase randomization. As shown in Fig. 2(b), the measured reflectivities for three different heights are lower than 3% up to an incident angle of 60° for p-polarization. It is worth noting that the reflectivities of nanopillars decrease as the incident angle increases before Brewster's angle, similar to those of bulk. Although Brewster's angle becomes indiscernible in nanopillar structures, minimal reflectivities occur at incident angles of 53.5°, 48.8°, and 46.4° for h=300, 550, and 720 nm, respectively, showing a linear correlation between the pillar height and the incident angle of the minimal reflectivity. This characteristic can also be observed in the measured reflectivity ratio of polarizations, that is, the ratio of the reflectivity of the s-polarization to that of the p-polarization, denoted as I_s/I_p. As shown in Fig. 3, the bulk GaN exhibits a calculated peak of $I_s/I_p > 10^4$ at Brewster's angle of 63.5°, while I_s/I_p drops significantly to <20 for all nanopillar structures. As the height of the nanopillar increases, the peak of I_s/I_p shifts towards a smaller incident angle. Figure 3 suggests that the reflectivities become polarization-insensitive even in a shallow nanostructured surface. It is also worth noting that the ratio I_s/I_p is enhanced at small incident angles, since the spatial symmetry of bulk at the normal incidence is altered by the nanostructures. Similar results have been observed in GaN nano-wires on sapphire with different coverage ratios [11].

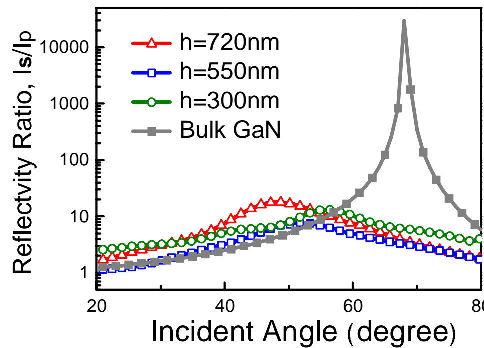

Fig. 3. The measured reflectivity ratio of polarizations, I_s/I_p for nanopillars of h=300, 550, and 720 nm is plotted as a function the incident angle, while that for bulk GaN is simulated for reference. The reflectivities of nanopillar structures are polarization-insensitive compared to those of bulk.

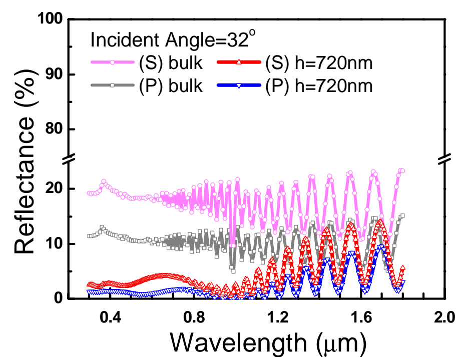

Fig. 4. The reflectivity spectroscopy for bulk GaN and the nanopillars with a height of 720 nm at an incident angle of 32°.

#92997 - $15.00 USD Received 28 Feb 2008; revised 29 Mar 2008; accepted 31 Mar 2008; published 30 May 2008
(C) 2008 OSA

The reflectivity spectroscopy with light incident at an angle of 32° is shown in Fig. 4. Bulk GaN exhibits reflectivities of ~23% for s-polarization and ~13% for p-polarization in the wavelength range between 300 nm and 1800 nm, while the GaN nanopillars of h=720 nm show reflectivities <5% in the 300-1200 nm wavelength range, and <10% in λ=1200-1800 nm for both polarizations.

The measured reflectivities of GaN nanopillars are about an order of magnitude smaller than those of the reported porous structures [2], suggesting additional AR mechanisms besides the porous structure effect. Since the SEM images show distinctive pillar profiles for the three samples, it is of great interest to understand whether the structural properties, such as the density, geometric shapes, and dimensions can contribute to the omnidirectional AR characteristics. Therefore, a theoretical model based on a RCWA method is developed to investigate the dependence of the AR characteristics on the structural properties of nanopillars.

The RCWA method is often employed to solve the diffraction and transmission efficiency of optical diffractive elements, where the reflectivity is obtained as a sum of the reflected diffraction efficiencies of different diffraction orders. In order to minimize the calculation errors arising from periodic boundary conditions in disordered structures, a unit-cell is defined with dimensions at least an order of magnitude larger than the incident wavelength. The size of unit cell and randomness of nanopillar positions have also been studied to ensure convergence. Calculations show that a refractive-index gradient between air (n=1) and bulk GaN (n=2.5) is the key element to significantly reduce the reflection. Physically speaking, this gradient does not have to be linear, as long as the increment in the refractive indices is small enough such that the incident light can hardly experience changes in the dielectric environment. Hence, the shape of nanopillars, which determines the refractive-index gradient, is desired to be cone-like or spearhead-like structures. The periodic SWS with shapes of pyramids are nearly ideal AR structures, since the nano-pyramids provide a linear gradient of the refractive indices between air and the silicon substrate [12]. In order to apply the design concept to disordered structures, we can define the fill factor as the ratio between the areas covered by nanopillars with respect to a unit cell. It is desirable that the fill factor at the base of the nanopillars approaches one while that at the top approaches zero. The comparison of the angular and spectral AR characteristics between periodic and random nanostructures is discussed in [13].

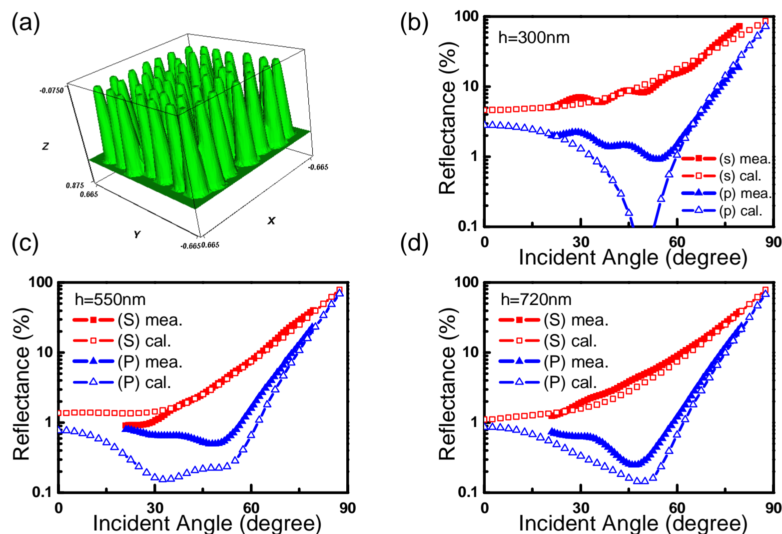

Fig. 5. (a). The index profile consists of 7x7 random nanopillars with a height of 720 nm. Calculated reflectivities of GaN nanopillars are plotted as a function of the incident angle for three different heights: (b) h=300 nm, (c) h=550 nm, and (d) h=720 nm, for both s- and p-polarizations.

#92997 - $15.00 USD Received 28 Feb 2008; revised 29 Mar 2008; accepted 31 Mar 2008; published 30 May 2008
(C) 2008 OSA

We first investigate the origins of the omnidirectional antireflection by fitting the measured data assuming a linear refractive-index gradient. The calculation is focused on the structural properties -- such as the refractive index gradient and the fill factors -- which can be collectively described and correlated to the AR characteristics. The randomness of pillar diameters and profiles is neglected in simulation because it provides little insight for the reduction of reflectivities, even though it does add fluctuations in the calculated reflectivities due to the finite unit cell size. Figure 5(a) shows the refractive-index profile of a unit cell, which consists of 7x7 random nanopillars with a height of 720nm. The unit cell has an area of ~1.6 μm^2, corresponding to a density of ~$3x10^9 cm^{-2}$. The top/bottom diameters of the pillars with h=300nm, 550nm, and 720nm are chosen to be 140/170, 100/180, and 80/190 nm, respectively. The calculated reflectivities of random nanopillars are plotted as a function of the incident angle in Fig. 5 for (b) h=300nm, (c) h=550nm, and (d) h=720nm. Although the index profiles used for fitting do not resemble the SEM images of the nanopillars microscopically, the calculations in Fig. 5 indicate that both structures share similar macroscopic AR characteristics. According to the nanopillar profiles shown in Fig. 1(c) for h=550nm and 1(d) for h=720nm, the collective index profiles exhibit a non-linear gradient which results in the omnidirectional AR characteristics. On the other hand, the AR properties for h=300nm are limited by the etch depth and the pillar profile.

Moreover, since the pillar height is directly related to the etching time, it is also desirable to investigate the correlations between the heights and the AR characteristics of disordered nanopillars. The calculation parameters for nanopillars of h=720nm are used for this study. In a process condition where the refractive-index gradient is fixed, we assume that the base fill factor changes with the pillar height, as shown in the inset of Fig. 6(a). The reflectivities of nanopillars are calculated as a function of pillar height at a light-incident angle of 21° with a fixed refractive-index gradient for both s- and p-polarizations. As shown in Fig. 6(a), the reflectivities drop to less than 2%, as the height becomes larger than 500 nm. However, in a situation where top and bottom fill factors are fixed and chosen to be close to zero and unity, respectively, the pillar height determines the refractive-index gradient, as illustrated in the inset of Fig. 6(b). The calculated reflectivities of both polarizations in this case quickly decrease to less than 2% as soon as the height is over 150nm. These calculations indicate that the design of AR nanostructures relies on the choices of fill factors and the refractive-index gradient from which the fabrication parameters, such as the density of Ni nano-masks and the etch depth can be derived.

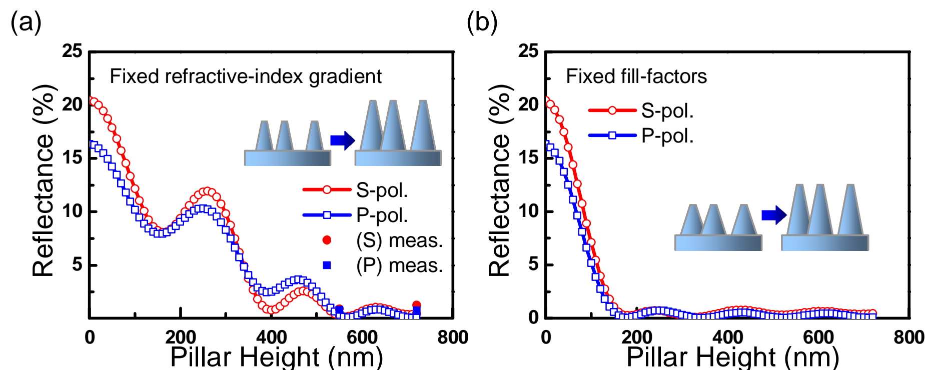

Fig. 6. The reflectivities of nanopillars are calculated as a function of pillar height (a) with a fixed refractive-index gradient, and (b) with fixed fill factors for both s- and p-polarizations at an incident angle of 21°.

4. Conclusion

We have investigated the angular and spectral reflectivities of GaN nanopillars with three different heights: h=300 nm, 550 nm and 720 nm. The nanopillar structures exhibit

#92997 - $15.00 USD Received 28 Feb 2008; revised 29 Mar 2008; accepted 31 Mar 2008; published 30 May 2008
(C) 2008 OSA

omnidirectional and broadband AR characteristics, up to an incident angle of 50° and 60° for s- and p-polarizations, respectively, and for the wavelength range of λ=300-1800nm. Moreover, the reflectivities of nanopillars are polarization-insensitive compared to those of bulk. Calculations based on a RCWA method reveals that the superior AR characteristics arise mainly from the refractive-index gradient profile provided by the nanopillars between air (n=1) and bulk GaN (n=2.5). The theoretical study concludes that the design of disordered AR nanostructures relies on the choices of the refractive index gradient and the fill factors from which the fabrication parameters can be obtained.

Acknowledgments

The authors would like to thank Prof. S. Lin at Rensselaer Polytechnic Institute for useful discussion. This work was supported by the National Science Council, Taiwan under grant number, NSC95-3114-P-009-001-MY2 and NSC96-2120-M009-006.

#92997 - $15.00 USD Received 28 Feb 2008; revised 29 Mar 2008; accepted 31 Mar 2008; published 30 May 2008
(C) 2008 OSA